J. Plasma Physics (2010), *vol.* 76, *parts* 3&4, *pp.* 419–428. © Cambridge University Press 2010
doi:10.1017/S0022377809990638

An electron model with elementary charge

B. LEHNERT and L. J. HÖÖK

School of Electrical Engineering, Div Fusion Plasma Physics, Royal Institute of Technology (KTH), Teknikringen 31, SE-100 44 Stockholm, Sweden
(bol@kth.se)

(Received 25 November 2009 and accepted 8 December 2009, first published online 25 January 2010)

Abstract. An earlier elaborated model of the electron, being based on a revised quantum electrodynamic theory, is further investigated in terms of an improved numerical iteration scheme. This point-charge-like model is based on the "infinity" of a divergent generating function being balanced by the "zero" of a shrinking characteristic radius. This eliminates the self-energy problem. According to the computations, the quantum conditions on spin, magnetic moment, and magnetic flux, plus the requirement of an elementary charge having the experimental value, can all be satisfied within rather narrow limits by a single scalar parameter. The revised model prevents the electron from "exploding" due to its eigencharge.

1. Introduction

The vacuum is not merely an empty space. According to quantum mechanics there is a nonzero level of the ground state, the zero point energy. With this as an incitement, a Lorentz and gauge invariant revised quantum electrodynamic theory has been based on the hypothesis of a nonzero electric field divergence in the vacuum state [1–5]. Due to this additional degree of freedom, a space-charge current arises in the resulting field equations, beside the displacement current. As compared to Maxwell's equations, new results and applications are then obtained, such as those of steady electromagnetic states and modified electromagnetic wave phenomena. An electron model further results from the steady states, having a net integrated electric charge. In the model relevant quantum conditions have been imposed on the angular momentum, on the magnetic moment and on the magnetic flux. From numerical computations an integrated electric charge was thereby deduced, which deviated by only a few percent from the experimental value "e" of the elementary charge. However, the parts of the computation related to the magnetic field geometry were connected with a complicated and rather tedious matching procedure thus becoming a source of numerical errors. This paper therefore describes a modified and improved iteration procedure, due to which the integrated charge and all related subsidiary conditions are treated with a high degree of accuracy.

2. Basic concepts of the electron model

Here the basic concepts of the present theory are shortly reviewed, whereas reference is made to earlier investigations [1–5] for the details. The basic field equations

https://doi.org/10.1017/S0022377809990638 Published online by Cambridge University Press

of a steady electromagnetic vacuum state become

$$\text{curl } \mathbf{B}/\mu_0 = \epsilon_0(\text{div } \mathbf{E})\mathbf{C}, \tag{2.1}$$

$$\mathbf{B} = \text{curl } \mathbf{A}, \tag{2.2}$$

$$\mathbf{E} = -\nabla\phi, \quad \text{div } \mathbf{E} = \bar{\rho}/\epsilon_0 \tag{2.3}$$

for the electric and magnetic fields $\mathbf{E}$ and $\mathbf{B}$, the corresponding potentials ϕ and $\mathbf{A}$, the electric charge density $\bar{\rho}$, and the dielectric constant ϵ_0 and magnetic permeability μ_0 in the vacuum. The vector $\mathbf{C}$ has a modulus equal to the velocity c of light.

For a model of the electron at rest, we study an axisymmetric state in a spherical frame (r, θ, φ) with $\mathbf{C} = (0, 0, C)$, $C = \pm c$ for the two spin directions, and $\mathbf{A} = (0, 0, A)$. Equations (2.1)–(2.3) then reduce to

$$\frac{(r_0\rho)^2\bar{\rho}}{\epsilon_0} = D\phi = \left[D + (\sin\theta)^{-2}\right](CA), \tag{2.4}$$

where $\rho = r/r_0$ with r_0 as a characteristic radial dimension, $D = D_\rho + D_\theta$ and

$$D_\rho = -\frac{\partial}{\partial\rho}\left(\rho^2\frac{\partial}{\partial\rho}\right), \quad D_\theta = -\frac{\partial^2}{\partial\theta^2} - \frac{\cos\theta}{\sin\theta}\frac{\partial}{\partial\theta}. \tag{2.5}$$

The solution of the system (2.4) is given by a *generating function*

$$F(r, \theta) = CA - \phi = G_0 \cdot G(\rho, \theta), \tag{2.6}$$

where G_0 stands for its amplitude and G for a normalized dimensionless part. This results in a general solution of the form

$$CA = -(\sin\theta)^2 DF, \quad \phi = -\left[1 + (\sin\theta)^2 D\right] F \tag{2.7}$$

$$\bar{\rho} = -\left(\frac{\epsilon_0}{r_0^2\rho^2}\right) D\left[1 + (\sin^2\theta)D\right] F. \tag{2.8}$$

With the definitions

$$f(\rho, \theta) = -(\sin\theta)D\left[1 + (\sin\theta)^2 D\right] G, \tag{2.9}$$

$$g(\rho, \theta) = -\left[1 + 2(\sin\theta)^2 D\right] G, \tag{2.10}$$

the integrated electric charge q_0, magnetic moment M_0, mass m_0, and angular momentum s_0 become

$$q_0 = 2\pi\epsilon_0 r_0 G_0 J_q, \qquad I_q = f \tag{2.11}$$

$$M_0 = \pi\epsilon_0 C r_0^2 G_0 J_M, \qquad I_M = \rho(\sin\theta)f \tag{2.12}$$

$$m_0 = \pi(\epsilon_0/c^2) r_0 G_0^2 J_m, \qquad I_m = fg \tag{2.13}$$

$$s_0 = \pi(\epsilon_0 C/c^2) r_0^2 G_0^2 J_s, \qquad I_s = \rho(\sin\theta)fg \tag{2.14}$$

with the normalized integrals

$$J_k = \int_{\rho_k}^{\infty}\int_0^{\pi} I_k \, d\rho \, d\theta, \quad k = q, M, m, s. \tag{2.15}$$

https://doi.org/10.1017/S0022377809990638 Published online by Cambridge University Press

In expression (2.15) $\rho_k \neq 0$ are small radii at the origin $\rho = 0$ when G is divergent there, and $\rho_k = 0$ when G is convergent at $\rho = 0$. The analysis is now restricted to a separable generating function $G = R(\rho)T(\theta)$. The integrals (2.15) then reduce to a separable form $J_k = J_{k\rho}J_{k\theta}$. An examination of the radial part R further yields the following results:

- For a convergent R at $\rho = 0$ the charge q_0 and magnetic moment M_0 vanish, regardless of the symmetry properties of T. This leads to a model of an electrically neutral particle, such as the neutrino.
- For a divergent R at $\rho = 0$, and for a polar part T being symmetric with respect to the mid-plane $\theta = \pi/2$, there are nonzero q_0 and M_0. This leads to a model of a charged particle, such as the electron.

The electron model with a divergent $R(\rho)$ and a symmetric $T(\theta)$ is then given by

$$R = \rho^{-\gamma} e^{-\rho}, \quad \gamma > 0, \tag{2.16}$$

$$T = 1 + \sum_{\nu=1}^{n} \{a_{2\nu-1} \sin[(2\nu-1)\theta] + a_{2\nu} \cos 2\nu\theta\}, \tag{2.17}$$

where $\gamma(\gamma-1) = 2+\delta, \quad 0 \leqslant \delta \ll 1$, and γ approaches the value 2 from above. With the notation $A_q = J_{q\theta},\ A_M = J_{M\theta}/\delta,\ A_m = J_{m\theta},\ A_s = J_{s\theta}$ and $\rho_q = \rho_M = \rho_m = \rho_s = \epsilon$, expressions (2.11)–(2.14) for the integrated field quantities become

$$q_0 = 2\pi\epsilon_0 r_0 G_0 A_q/\epsilon, \tag{2.18}$$

$$M_0 m_0 = \pi^2 \epsilon_0^2 (C/c^2)(r_0 G_0)^3 A_M A_m/\epsilon^3, \tag{2.19}$$

$$s_0 = \frac{1}{2}\pi(\epsilon_0 C/c^2)(r_0 G_0)^2 A_s/\epsilon^2, \tag{2.20}$$

where

$$A_q = -3.141592654a_3 - 2.400000000a_2 - 1.333333333 + 1.714285714a_4, \tag{2.21}$$

$$\begin{aligned} A_M = {} & -.7853981635a_2 - 2.171428571a_3 + .8507936508a_5 \\ & + 1.963495409a_4 - 1.333333333a_1 - 2.356194491, \end{aligned} \tag{2.22}$$

$$\begin{aligned} A_m = {} & 54.97142857a_2^2 + 723.7448773a_3^2 - 3251.548397a_3a_4 + 367.5663405a_2a_3 \\ & - 67.42857143a_4 + 15409.51197a_4a_5 + 50.26548246a_3 + 3.466666667 \\ & + 21.25714286a_2 - 707.8441558a_2a_4 + 4231.268731a_4^2 - 933.0530182a_5a_2 \\ & - 5070.283317a_5a_3 - 56.54866777a_5 + 16357.19800a_5^2, \end{aligned} \tag{2.23}$$

$$\begin{aligned} A_s = {} & -109.3010101a_5 + 343.5520924a_2a_3 + 644.4468463a_3^2 + 2.057142857a_1a_2 \\ & + 5.497787145a_1a_3 + 49.48008430a_2^2 + .5333333333a_1 + 62.95873016a_3 \\ & - 8a_1a_4 - 3034.300278a_3a_4 - 102.1017613a_4 + 38887.720909a_4^2 \\ & - 1006.220979a_5a_2 - 699.7897637a_2a_4 + 15041.94563a_5^2 + 14374.48791a_4a_5 \\ & + 21.99114858a_2 + 3.141592654 - 4960.574801a_5a_3 - 7.068583472a_1a_5 \end{aligned} \tag{2.24}$$

https://doi.org/10.1017/S0022377809990638 Published online by Cambridge University Press

with values given for the first five amplitudes of the expansion (2.17). As will be seen later, only the combined expression for $M_0 m_0$ will be needed in the following analysis. The magnetic flux Ψ is obtained from the first part of (2.7). At the corresponding normalized radius $\rho = \rho_\Gamma = \epsilon$, the normalized flux function becomes

$$\Psi \equiv \Gamma(\rho = \epsilon, \theta)/2\pi(r_0 G_0/\epsilon C) = \sin^3\theta(D_\theta T - 2T)$$

$$= -(a_1 + 3a_3 + 5a_5)s^2 + (-2 + 6a_2 + 30a_4)s^3 + (36a_3 + 180a_5)s^4$$

$$- (8a_2 + 160a_4)s^5 - (40a_3 + 600a_5)s^6 + 144a_4 s^7 + 448a_5 s^8 + \cdots , \quad (2.25)$$

where $s \equiv \sin\theta$. In the cases to be treated here, the radial magnetic field component is found to vanish at the angles $\theta = \theta_1$ and $\theta = \theta_2$ within the range $0 \leqslant \theta \leqslant \pi/2$. These angles represent the two zero points of the derivative $d\Psi/ds$ of the flux function (2.25). When θ increases from $\theta = 0$ at the axis, the flux Ψ first increases to a maximum at θ_1. Then follows an interval $\theta_1 \leqslant \theta \leqslant \theta_2$ of decreasing flux, down to a minimum at θ_2. Finally, in the range $\theta_2 \leqslant \theta \leqslant \pi/2$, the flux increases again, up to the total main value

$$\Psi_0 = \Psi(\pi/2) \equiv A_\Gamma = -2 - a_1 - 2a_2 - 7a_3 + 14a_4 + 23a_5 + \cdots . \quad (2.26)$$

This behavior is due to a magnetic island having dipole-like field geometry with current centra at θ_1 and θ_2. Thus the total flux includes the main part (2.26), plus that from two magnetic islands at each side of the mid-plane $\theta = \pi/2$. It becomes

$$\Psi_{tot} = f_\Gamma \Psi_0, \quad f_\Gamma = 1 + 2\left[\Psi(s_1) - \Psi(s_2)\right]/\Psi_0. \quad (2.27)$$

Here f_Γ is the corresponding flux factor, where the unity term stands for the main flux and the rest for the contribution from the magnetic islands. Three quantum conditions have to be imposed. First, the angular momentum (spin) s_0 has to take the values $\pm h/4\pi$. With the definition $q^* = |q_0/e|$, where e is the experimental value if the elementary charge, this condition reduces to

$$q^* = (f_0 A_q^2/A_s)^{1/2}, \quad f_0 = 2\epsilon_0 ch/e^2, \quad (2.28)$$

where f_0 is the inverted value of the fine-structure constant. Second, the magnetic moment is subject to a condition formulated by Dirac [6], Schwinger [7], and Feynman [8]. It reduces to the relation

$$A_M A_m / A_q A_s = 1 + \delta_M, \quad \delta_M = 1/2\pi f_0 = 0.0011614. \quad (2.29)$$

Third, the total magnetic flux has to become quantized, by being equal to the ratio $|s_0/q_0|$, i.e.

$$8\pi f_\Gamma A_\Gamma A_q = A_s. \quad (2.30)$$

Here we observe that all three conditions (2.28)–(2.30) become independent of the parameter $r_0 G_0/\epsilon$, which appears in (2.18)–(2.20) and in (2.25).

In conventional theory there is only an unbalanced radial electrostatic force due to the electron charge, and this tends to "explode" the configuration [9]. However, using well-known vector identities in the present case of (2.1)–(2.3), the volume force density becomes

$$f = \bar{\rho}(\mathbf{E} + \mathbf{C} \times \mathbf{B}) \quad (2.31)$$

https://doi.org/10.1017/S0022377809990638 Published online by Cambridge University Press

having an additional magnetic term $\mathbf{C} \times \mathbf{B}$. The integrated radial force is given by

$$F_r = 2\pi \int \int f_r r^2 \sin\theta \, dr \, d\theta = J_R J_T . \tag{2.32}$$

A recent deduction of this force [10] can shortly be summarized as follows. As shown earlier, an electron model requires the radial part (2.16) of the separable generating function (2.6) to be divergent at the origin, and be restricted to $\gamma = 2$. Addition of an extra term in the radial part having $\gamma = 1$ does not contribute to the charge density. The distribution of the latter further includes the boundary condition of being zero within the hollow region $\rho < \epsilon$ near the origin. Taking this into account, the radial factor J_R is always negative. The polar factor J_T is given by

$$J_T = \int_0^\pi f_\rho e_\rho \, d\theta. \tag{2.33}$$

Here positive values of J_T result in a negative F_r and in a tendency to "implode" the configuration, whereas a negative J_T tends to "explode" the latter. The detailed force balance in the case of a positive J_T is likely to be quite a complicated problem which is not treated in this paper. After a number of deductions based on (2.8), (2.3), (2.7), and (2.2), the functions f_ρ and e_ρ become

$$\begin{aligned} f_\rho &= 2sT - 4s^3T - sD_\theta T + 2s^3 D_\theta T + 2sD_\theta(s^2T) - sD_\theta(s^2 D_\theta T) \\ &= (18a_2 + 90a_4)s + (288a_3 + 1440a_5)s^2 - (144a_2 + 2520a_4)s^3 \\ &\quad - (1320a_3 + 16200a_5)s^4 + (144a_2 + 7920a_4)s^5 + (1120a_3 + 38304a_5)s^6 \\ &\quad - 5760a_4 s^7 - 24192a_5 s^8 + \cdots , \end{aligned} \tag{2.34}$$

$$\begin{aligned} e_\rho &= -2T + 2s^2T - s^2 D_\theta T \\ &= -(2a_2 + 2a_4) - (a_1 + 3a_3 + 5a_5)s - (2a_2 + 14a_4)s^2 \\ &\quad - (28a_3 + 140a_5)s^3 + (8a_2 + 144a_4)s^4 + (40a_3 + 568a_5)s^5 \\ &\quad - 144a_4 s^6 - 448a_5 s^7 + \cdots . \end{aligned} \tag{2.35}$$

In earlier deductions of (2.34) there was a miscalculation of the term $7920a_4 s^5$, having instead the coefficient 8727.

3. Earlier numerical analysis

The elementary electronic charge has so far been considered as an independent constant of nature, determined by measurements. Since it appears to represent the smallest quantum of free electric charge, however, the question can be raised whether it could result from a quantized variational analysis. In a first attempt such an analysis has been applied, as based on the present theory and with the subsidiary quantum conditions in terms of Lagrangian multipliers. This attempt failed, because there was no well-defined and localized point of an extremum [5]. An alternative approach was then applied in which the study was limited to the first four amplitudes of the expansion (2.17), the quantum conditions (2.28)–(2.30)

https://doi.org/10.1017/S0022377809990638 Published online by Cambridge University Press

were imposed, and q^* was plotted as a function of a_3 and a_4, which were scanned across their entire ranges of variation. For real q^* the result was as follows [5]:

- Two real solutions were found. That with the lowest value of q^* was of main interest, and only this solution will henceforth be discussed here in detail.
- In a range of $a_3 \leqslant 0$ and $a_4 \leqslant 0$ a "barrier" was found within which q^* dropped from values $q^* \gg 1$ down to a level close to $q^* = 1$.
- In the ranges of $a_3 \gg 1$ and $a_4 \gg 1$ the values of q^* were localized to a flat "plateau" within which q^* deviated only by a few percent from the experimental value $q^* = 1$. This explained the failure of the variational analysis.

To calculate the plateau values of q^*, including the magnetic flux condition (2.30) and the varying magnetic flux factor (2.27), a rather tedious matching procedure was applied, which resulted in values of q^* that deviated only by some percent from the experimental one [2, 3]. However, this procedure included numerical errors.

4. An improved numerical iteration scheme

Within the plateau region, where all amplitudes $(a_1, a_2, a_3, \ldots)$ in (2.21)–(2.26), (2.34) and (2.35) take large values, an improved iteration scheme has been proposed [10]. The auxiliary parameters

$$h_0 = \bar{A}_m / \bar{A}_s, \quad g_0 = \bar{A}_s / 8\pi \bar{A}_\Gamma f_\Gamma \tag{4.1}$$

are first introduced, where a bar indicates the limit of large amplitudes. Then the two quantum conditions (2.29) and (2.30) are written as

$$h_0 \bar{A}_m = (1 + \delta_M)\bar{A}_q, \quad \bar{A}_q = g_0 \tag{4.2}$$

with the notations

$$x = a_1/a_\infty, \; y = a_2/a_\infty,$$

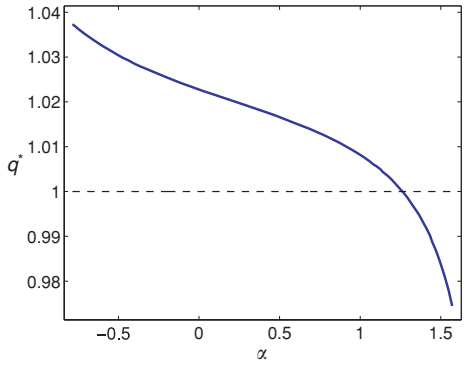
$$a = a_3/a_\infty = -\sin\alpha, \; b = a_4/a_\infty = \cos\alpha \tag{4.3}$$

and $c_\mu = a_\mu/a_\infty$, $(\mu = 5, 6, \ldots)$, $a_\infty \gg 1$ being introduced. Relevant values of α in the plateau region of the four-amplitude case [3, 5] correspond to the range $-\pi/4 \leqslant \alpha \leqslant \pi/2$. With given values for each of the normalized amplitudes (a, b, c_μ), expressions (4.2) then form a simple linear system of equations for the variables x and y. The iteration procedure begins with adopted values of h_0 and g_0, and end with self-consistent values satisfying the quantum conditions (2.29) and (2.30). As a consequence of the obtained solution, corresponding values of q^* and J_T are then obtained according to (2.28) and (2.33). We finally observe that, in the plateau region, all factors (2.21)–(2.24) have quadratic forms of the amplitudes in the expansion (2.17). In the four-amplitude case the quantum conditions (2.28)–(2.30) therefore depend on the angle α only, and not on the magnitude of $a^2 + b^2$.

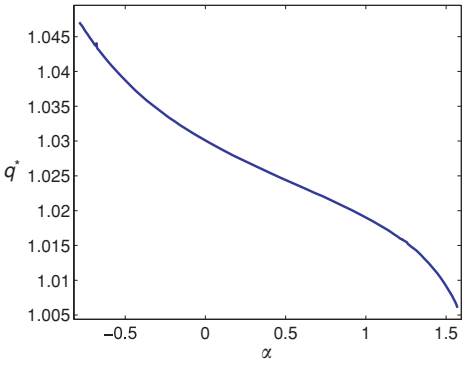
5. Numerical analysis

In a determination of the deduced normalized charge q^* the present theory relies on the three quantum conditions (2.28)–(2.30). The disposable independent variables are the amplitudes $(a_1, a_2, a_3, \ldots)$. In all cases up to five amplitudes, the iteration scheme of Sec. 4 was found to converge rapidly, after about seven iterations. When limiting the analysis to the first four amplitudes, the three quantum conditions will specify the charge q^* as a function of the angular variable α at the perimeter

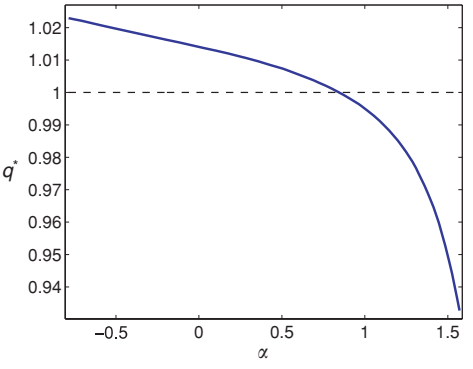
https://doi.org/10.1017/S0022377809990638 Published online by Cambridge University Press



(a)



(b)



(c)

Figure 1. (Color online) The normalized charge $q* = |q_0/e|$ as a function of the angle α at the perimeter of the plateau: (a) four amplitudes only, (b) five amplitudes with $c_5 = 0.05$, (c) five amplitudes with $c_5 = -0.05$.

of the plateau region, with the notations (4.3). The behavior of the normalized charge is then demonstrated by Fig. 1(a). In the plateau region corresponding to the range $-0.8 \leqslant \alpha \leqslant 1.6$, this charge was found to be bound within the limits $1.04 \geqslant q^* \geqslant 0.97$, i.e. with a deviation of only a few percent from the experimental value $q^* = 1$. The latter value was reached at the angle $\alpha \cong 1.26$. The addition of a small contribution from a fifth amplitude changes this result dramatically. This is

https://doi.org/10.1017/S0022377809990638 Published online by Cambridge University Press

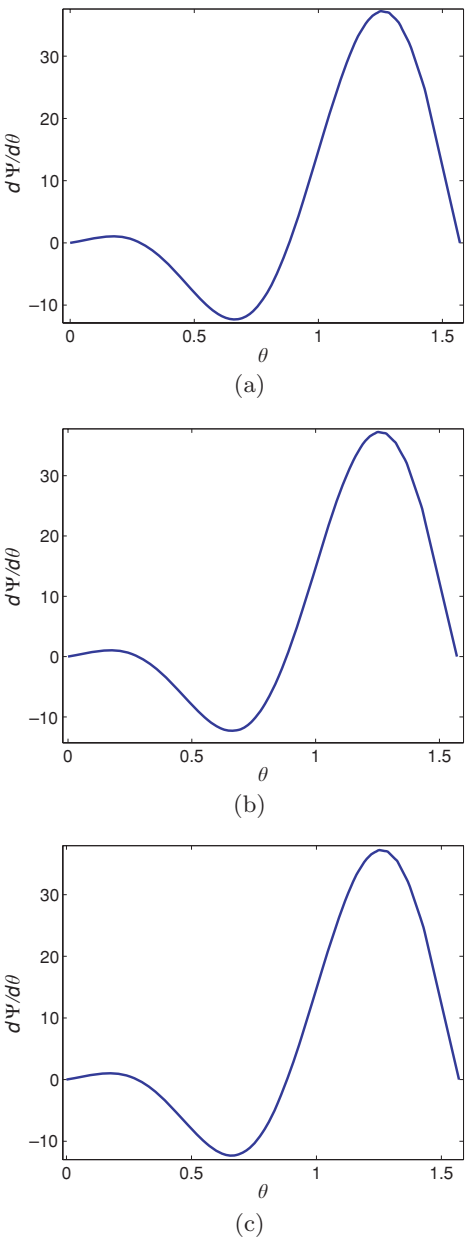


Figure 2. (Color online) The normalized magnetic flux $d\Psi/d\theta$ per unit angle θ, with $\alpha \approx 1.26$ for which $q^* = 1$ in the four amplitude case: (a) four amplitudes only, (b) five ampltidues with $c_5 = 0.05$, (c) five amplitudes with $c_5 = -0.05$.

shown in Fig. 1(b) for $c_5 = 0.05$ where there is no value of α satisfying the condition $q^* = 1$, and in Fig. 1(c) for $c_5 = -0.05$ where the value of α for $q^* = 1$ has been displaced from $\alpha = 1.26$ to $\alpha = 0.80$.

The derivative $d\Psi/d\theta$ of the magnetic flux function (2.25) has been plotted in Fig. 2(a). Here the sum of the areas above the horizontal axis represents the total

https://doi.org/10.1017/S0022377809990638 Published online by Cambridge University Press

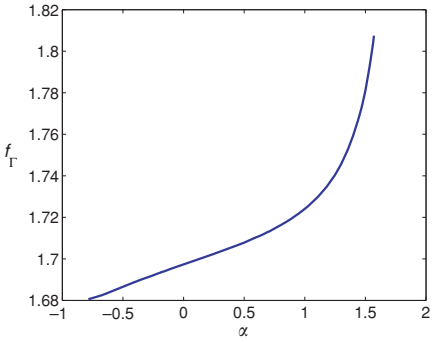


Figure 3. (Color online) The variation of the magnetic flux factor f_Γ in the four-amplitude case, as a function of the plateau angle α.

outflux in the upper half plane, whereas the area below the same axis represents the counter-directed flux due to one magnetic island. A comparison between Figs 2(a)–(c) reveals that there are also noticeable changes in the magnetic geometry when small contributions from the amplitude c_5 are included. The variation of the magnetic flux factor (2.27) with the angle α is further demonstrated in Fig. 3 of the four-amplitude case. Finally, the polar factor J_T of (2.33) has been plotted in Fig. 4(a), thus resulting in positive values within the entire region of α. This indicates that there is an inward directed confining radial integrated force, which tends to "implode" the electron configuration. To demonstrate the influence of the magnetic contribution $\mathbf{C} \times \mathbf{B}$ to the Lorentz force (2.31), a simulation has been performed in Fig. 4(b) where this contribution has been dropped. The sign of J_T' then becomes reversed, indicating that the system would "explode".

6. Summary and conclusion

As being stated earlier [2, 3], the present electron model is for a nonzero net electric charge forced is to have the character of a point-charge-like geometry. Here the "infinity" of a divergent generating function is balanced by the "zero" of a shrinking characteristic radius appearing in a finite parameter $r_0 G_0/\epsilon$ of (2.18)–(2.20) and (2.25). This eliminates the self-energy problem and provides a physically more acceptable alternative to the renormalization process in which extra ad hoc counter terms are added to the Lagrangian, to outbalance one "infinity" by another. The improved numerical analysis of this paper shows that the relevant basic properties of the electron can be reproduced by the present model. Thus, the three quantum conditions, plus the requirement to make the deduced elementary charge equal to the experimental value, can all be satisfied by merely adjusting one single scalar parameter, α. This further takes place within a narrow range of possible variations, where q^* only deviates by a few percent from the experimental value. Even small contributions from amplitude parameters in addition to the four first ones strongly modify the result and prevent a matching to the experimental value. Finally, due to the magnetic part of the Lorentz force, the present electron model is prevented from "exploding" under the influence of its eigencharge. This leads on the other hand to an inward directed integrated force, the balance of which requires further investigation.

https://doi.org/10.1017/S0022377809990638 Published online by Cambridge University Press

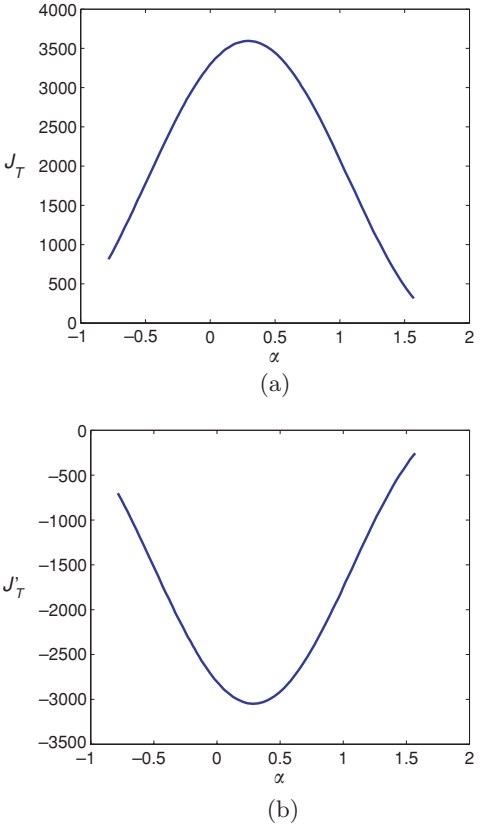


Figure 4. (Color online) The polar factor of the integrated radial force in the four-amplitude case: (a) polar factor J_T due to the full Lorentz force, (b) simulated reduced polar factor J'_T without the magnetic part of the Lorentz force.

References

[1] Lehnert, B. 1994 *Speculat. Sci. Tech.* **17**, 259.

[2] Lehnert, B. 2008 In: *New Aspects of Plasma Physics: Proceedings of the 2007 ICTP Summer College on Plasma Physics* (ed. P. K. Shukla, L. Stenflo and B. Eliasson). Singapore: World Scientific, p. 282.

[3] Lehnert, B. 2008 *A Revised Electromagnetic Theory with Fundamental Applications* (ed. D. Rabounski). Stockholm: Swedish Physics Archive; and (ed. A. Zagorodny and Z. I. Vakhnenko). Kiev: Bogoljubov Institute for Theroretical Physics.

[4] Lehnert, B. and Roy, S. 1998 *Extended Electromagnetic Theory*. Singapore: World Scientific.

[5] Lehnert, B. and Scheffel, J. 2002 *Phys. Scri.* **65**, 200.

[6] Dirac, P. A. M. 1928 *Proc. Roy. Soc.* **117**, 610 and **118**, 351.

[7] Schwinger, J. 1949 *Phys. Rev.* **76**, 790.

[8] Feynman, R. P. 1990 *QED: The Strange Theory of Light and Matter*. London: Penguin.

[9] Jackson, J. D. 1962 *Classical Electrodynamics*. New York: John Wiley & Sons, Inc., ch. 17.4, p. 589.

[10] Lehnert, B. 2009 Alfvén Laboratory, Royal Institute of Technology, Stockholm, Laboratory Report, unpublished.

https://doi.org/10.1017/S0022377809990638 Published online by Cambridge University Press